

Influence of Composition and Thermal Treatments on Microhardness of the Filled Skutterudite $\text{Sm}_y(\text{Fe}_x\text{Ni}_{1-x})_4\text{Sb}_{12}$

Cristina Artini^{1,2,*} and Riccardo Carlini^{1,3}

¹DCCI, Department of Chemistry and Industrial Chemistry, University of Genova, Genova, 16146, Italy

²CNR-ICMATE, Genova, 16149, Italy

³INSTM, Genova Research Unit, Genova, 16146, Italy

Samples belonging to the series $\text{Sm}_y(\text{Fe}_x\text{Ni}_{1-x})_4\text{Sb}_{12}$ were heated in Ar atmosphere up to 400 °C and cooled down to room temperature several times, with the aim to evaluate the effect of thermal cycles on microhardness. The treatment temperature was chosen in correspondence of the maximum ZT value, in order to simulate the operating conditions of the material in a thermoelectric device. Vickers measurements allowed to detect the effect of both composition and thermal treatments on the microhardness properties of the material. A decrease in the microhardness value was observed prior to thermal treatments with increasing Fe amount, due to the substitution of Ni by the larger Fe atom. Moreover, almost all compositions show an increase in the hardness of the skutterudite phase as a consequence of thermal cycles, accounting for the Sb enrichment of skutterudite. This evidence suggests also a possible improvement of the preparation procedure in order to obtain a stoichiometric Sb amount within the skutterudite. Samples were prepared by direct reaction of pure elements at 950 °C followed by thermal treatment at 620 °C. The composition and microstructure of the obtained samples were investigated by X-ray powder diffraction, and by optical and electronic microscopy.

Keywords: Thermoelectric Materials, Skutterudites, Electronic Microscopy, Microhardness, Thermal Treatments.

1. INTRODUCTION

Among the materials currently studied in view of thermoelectric applications, such as clathrates,¹ tetrahedrite,² and skutterudite-related³ intermetallic compounds, filled skutterudites form an interesting family of materials because of the tunability of their electronic properties.^{4,5} They can be considered as formally derived from the parent skutterudite CoSb_3 by partial substitution of Co with another metal (such as, for example, Fe), or by total removal in favor of a mixture of two different transition elements (such as, for example, Fe/Ni). Since skutterudites can be conveniently described as Zintl's compounds, the replacement of Co by a lighter element leads to an electronic imbalance that needs to be recovered by the insertion of a further cation into the structure. The compensation generally takes place by introduction of a rare earth atom or by Ba^{2+} , that

provide the missing electrons, into the icosahedral cavity located in (0, 0, 0). As it is in general not possible to fully compensate electron deficiency by filling, *p*-type skutterudites occur, characterized by an electronic amount lower than the one of the parent compound. By substitution of Co by a mixture Fe/Ni, the electron deficiency or abundancy can be modulated by tuning the Fe/Ni ratio, so giving rise to *n*- or *p*-type skutterudites. By means of this phenomenological approach, it was possible to synthesize and to study the physical properties of a large number of filled skutterudites, such as $\text{Ce}_y\text{Fe}_{4-x}\text{Co}_x\text{Sb}_{12}$,⁶ $\text{Yb}_y\text{Fe}_{1.5}\text{Co}_{2.5}\text{Sb}_{12}$,⁷ $\text{Yb}_y\text{Fe}_2\text{Ni}_2\text{Sb}_{12}$,⁸ $\text{Ce}_y\text{Fe}_{4-x}\text{Ni}_x\text{Sb}_{12}$,^{9,10} $\text{Sm}_y\text{Fe}_{4-x}\text{Ni}_x\text{Sb}_{12}$,^{11,12} $\text{Mm}_y\text{Fe}_{4-x}(\text{Co},\text{Ni})_x\text{Sb}_{12}$ (Mm: mischmetal)¹³ and $(\text{Ce},\text{Yb})_y\text{Fe}_{4-x}(\text{Co},\text{Ni})_x\text{Sb}_{12}$.¹⁴ High values of the figure of merit ZT of filled skutterudites (for instance, $\text{ZT} = 1.25$ at 630 °C for $\text{Ba}_{0.3}\text{Ni}_{0.05}\text{Co}_{3.95}\text{Sb}_{12}$ ¹⁵ and $\text{ZT} = 1.1$ at 480 °C for $\text{Ce}_{0.28}\text{Fe}_{1.52}\text{Co}_{2.48}\text{Sb}_{12}$ ¹⁶) are due to the presence of the

*Author to whom correspondence should be addressed.

dopant ion within the icosahedral cage, that through its rattling movement lowers the phononic contribution to thermal conductivity.

Skutterudites MX_3 crystallize in a body-centered cubic cell (Pearson symbol $cI32$, isotypic crystal: CoAs_3 , space group: $Im\bar{3}$), with M and X occupying the $8c$ ($1/4, 1/4, 1/4$) and the $24g$ ($0, y, z$) atomic sites, respectively.¹⁷ As a consequence of the atomic arrangement, the aforementioned X_{12} icosahedral cavity is formed in position $2a$ in $(0, 0, 0)$. If all the voids are filled, the composition of a filled skutterudite, $\text{M}_4\text{X}_{12}\text{RE}$ (RE \equiv rare earth), is obtained.¹⁸ The effects on the skutterudite structure of the filling by a foreign ion have been widely studied in several papers.^{12, 19}

A thermoelectric couple consists in a p - and an n -type leg connected via wires made of a good electrical conductor to build an electrical circuit. It is thus generally convenient to employ p - and n -legs obtained from the same matrix, so that the mismatch between coefficients of lattice thermal expansion, and in general between mechanical properties, are reduced as much as possible. Filled skutterudites offer the opportunity to change the conduction mechanism by tuning the ratio of the transition metals, and consequently the amount of the dopant ion; the effect of the Fe/Ni ratio variation in $\text{Sm}_y(\text{Fe}_x\text{Ni}_{1-x})_4\text{Sb}_{12}$ on the electronic properties of the material is thoroughly discussed in Ref. [12].

For the aforementioned reasons, and because of the need for mechanically reliable devices, the study of mechanical properties of filled skutterudites is of primary importance. The investigation of thermal expansion coefficients, hardness and elastic properties has been performed for several compositions by Rogl et al.,^{20, 21, 22} as well as by other groups.²³ Nevertheless, to our knowledge, mechanical properties of compositions belonging to the $\text{Sm}_y(\text{Fe}_x\text{Ni}_{1-x})_4\text{Sb}_{12}$ series have not ever been studied.

With the aim to follow the behaviour of microhardness of the filled skutterudite $\text{Sm}_y(\text{Fe}_x\text{Ni}_{1-x})_4\text{Sb}_{12}$ in experimental conditions similar to the operating ones, in this work tests have been performed on the as-prepared samples, as well as on samples submitted to thermal cycles at 400 °C; the treatment temperature has been chosen in the close vicinity of the maximum ZT value observed in these samples.¹¹ The trend of measured values as a function of thermal cycles is believed to result from the competition between the softening effect related to the grain enlargement deriving from the thermal treatments, and the hardening effect due to the Sb enrichment of the skutterudite phase. An effect of the Fe substitution by Ni on the microhardness values is observed, too.

2. EXPERIMENTAL DETAILS

2.1. Synthesis

Samples of composition $\text{Sm}_y(\text{Fe}_x\text{Ni}_{1-x})_4\text{Sb}_{12}$ ($x = 0.4, 0.56, 0.58, 0.63, 0.80, 0.90, 1$) were synthesized, as

described in Ref. [12], by direct reaction of pure elements Fe (Alfa-Aesar, 99.99 wt.%), Ni, Sm (NewMet, 99.9 wt.%) and Sb (Mateck, 99.99 wt.%). Sb was added in slight excess taking into account its high vapour pressure. The starting mixture was placed into an Ar-filled silica ampoule and subsequently sealed under an Ar flow. The tube was heated up to 950 °C for 3 hours and then quenched in an iced water bath; afterwards, samples were annealed at 600 °C for 4 days. Powders obtained by grinding annealed samples were sieved through a 44 μm sieve and analyzed by means of a Bragg-Brentano powder diffractometer (Philips PW1050/81, Fe-filtered $\text{Co K}\alpha$ radiation) making use of a zero-background sample holder in the range 15°–120°.

Five of the so obtained samples (the ones at $x = 0.4, 0.56, 0.58, 0.77$ and 0.90) were put into a sealed Ar-filled ampoule and submitted to three 24-hour lasting thermal treatments at 400 °C. After each cycle, samples were extracted from the furnace, quickly cooled and analyzed. Samples are hereafter named Fe90-1, Fe90-2, ..., according to the nominal % Fe content with respect to the total (Fe + Ni) amount, and to the number of thermal cycles.

2.2. Characterization

Micrographically polished surfaces of all the samples were observed by optical microscopy before and after etching with a 50 vol.% HNO_3 solution in ethanol; samples were analyzed prior to thermal cycles (unetched) and after the last cycle (etched) by Scanning Electron Microscopy (SEM) equipped with Energy Dispersive X-ray Spectroscopy (EDS) (Zeiss EVO 40, with Oxford Instruments Pentafet Link, software package: Oxford-INCA v. 4.07, standard: Co., acceleration voltage: 20 kV, working distance: 12 mm, live time: 40 s). Photos were taken both by backscattered and secondary electrons, and EDS analyses were performed on at least five points or areas to identify the phases and determine the local composition.

Microhardness measurements were carried out by means of a Leica VMHT microhardness tester provided with Vickers indenter on unetched samples prior to thermal cycles and after each cycle. In particular, tests were performed on all the as-prepared samples and on the five samples submitted to the thermal cycles. A test load of 50 g was applied with a dwell time of 15 seconds; 18–20 tests were performed on each sample. Indentations were done at random positions on the samples surface, in order to obtain a rough estimation about the occurrence of each phase. For sake of comparison, tests were done also on the polished surface of a Sb piece, and on some selected Sb grains visible on etched samples. The so obtained microhardness data were divided into distribution frequencies characterized by a width of 30 HV, that allowed to recognize the clusterization of data around some specific values, as described in the following section. Errors coupled to hardness average values correspond to the standard deviation.

3. RESULTS AND DISCUSSION

3.1. Composition and Microstructure

SEM-EDS analyses, as well as X-ray diffraction, show that all the analyzed samples are mainly composed of the skutterudite phase, and that the evaluated Fe/Ni ratio is very close to the nominal value; nevertheless, a certain amount of unreacted Sb can be recognized by both techniques, and traces of other additional phases [(Fe,Ni)Sb₂, (Fe,Ni)SmSb₃] are detected by EDS. In Figure 1 the diffractogram of sample Fe90-0 is shown: *hkl* indexes are associated to each peak of the main phase, and peaks related to the presence of Sb are indicated by an asterisk. In Table I the refined compositions (obtained by EDS analyses coupled to Rietveld refinements, as described in Ref. [12]), as well as the additional phases, are listed for each sample. The presence of a certain amount of unreacted Sb can be expected, due to the introduction of a slight excess of this element in the starting mixture, as previously described; nevertheless, the incomplete occupancy factor of the Sb atomic site deriving from refinements (see for example, in Table I, the refined composition of samples Fe90-0, Fe63-0 and Fe60-0), suggests that the synthesis procedure does not always guarantee the formation of a stoichiometric skutterudite.

The Sm amount that enters the structure is strictly related to the Fe/Ni ratio, and decreases with decreasing the Fe amount.

The presence of Sb is clearly visible both in optical and in electronic images, as evident from Figures 2(a and b), where the optical picture of Fe40-0 and the electronic one of Fe100-0 unetched samples are shown, respectively. Sb grains appear as islands with well-defined shapes, suggesting that they are located at the skutterudite grain boundaries. This idea is confirmed by Figure 2(c), where an electronic micrograph of the etched surface of sample 33-3 is shown: in the centre of the picture a wide area appears consisting of a strongly etched Sb-based solid solution (according to EDS analyses performed on the shown region, Sb dissolves ~1 at.% Ni), and a skutterudite grain growing within this matrix. The presence of Sb among skutterudite grains is strictly related to the synthetic

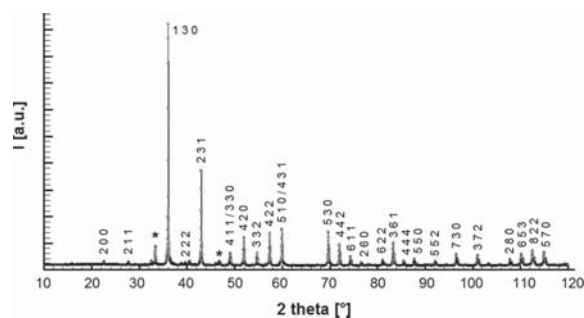


Figure 1. Diffraction spectrum of sample Fe90-0; *hkl* indexes of the skutterudite peaks are reported. Peaks of Sb are marked by asterisks (*).

Table I. Refined compositions and list of additional phases.

Sample	Refined composition	Additional phases
Fe100-0	$\text{Sm}_{0.78}\text{Fe}_{3.8}\text{Sb}_{12}$	Sb, FeSb ₂ , SmSb ₂ (traces)
Fe90-0	$\text{Sm}_{0.65}\text{Fe}_{3.3}\text{Ni}_{0.4}\text{Sb}_{11.7}$	Sb, (Fe,Ni)Sb ₂ (traces), SmSb ₂ (traces)
Fe80-0	$\text{Sm}_{0.54}\text{Fe}_{3.1}\text{Ni}_{0.9}\text{Sb}_{12}$	Sb, (Fe,Ni)Sb ₂ (traces)
Fe63-0	$\text{Sm}_{0.31}\text{Fe}_{2.5}\text{Ni}_{1.5}\text{Sb}_{11.6}$	(Ni,Fe,Sm)Sb ₂ (traces)
Fe60-0	$\text{Sm}_{0.23}\text{Fe}_{2.2}\text{Ni}_{1.6}\text{Sb}_{11.4}$	(Fe,Ni)Sb ₂ (traces)
Fe58-0	$\text{Sm}_{0.22}\text{Fe}_{2.1}\text{Ni}_{1.7}\text{Sb}_{12}$	Sb, SmSb ₂ , (Fe,Ni)Sb ₂ (traces)
Fe40-0	$\text{Fe}_{1.6}\text{Ni}_{2.2}\text{Sb}_{12}$	Sb

process, that consists in the heating of the starting mixture of elements up to 950 °C, aiming at the obtainment of a [Sb + (Fe,Ni)Sb₂ or (Fe,Ni,Sm)Sb₂] mixture, followed by the subsequent peritectic reaction at ~620 °C between the cited antimonides and the Sb-based liquid phase. As a consequence, antimony not contributing to the skutterudite formation is trapped during solidification at the skutterudite grain boundary. It is worth to underline that, according to EDS analyses, Sb appearing as additional phase dissolves a small but not negligible amount (up to 5 at.%) of Fe or Ni, that is expected to promote the phase hardening.

3.2. Microhardness

Microhardness measurements were performed on unetched samples, with the aim to obtain a statistical distribution of values, accounting for the distribution of the phases occurring in the samples. Indeed, for each composition the results of the tests mainly cluster around two values, located at about 500 HV and 350 HV, with distribution frequencies remarkably higher for the former. In few samples a third distribution centred at about 120 HV, and characterized by low frequency, is observed too.

According to Rogl et al.,²⁰ Vickers hardness values of Fe/Ni-based filled skutterudites are observed around 550 HV ($\text{HV}_{0.1} = 540 \pm 18$ for $\text{Ba}_{0.09}\text{Sr}_{0.02}\text{DD}_{0.22}\text{Yb}_{0.02}\text{Fe}_{2.4}\text{Ni}_{1.6}\text{Sb}_{12}$ and $\text{HV}_{0.1} = 560 \pm 20$ for $\text{Ba}_{0.15}\text{Yb}_{0.05}\text{DD}_{0.28}\text{Fe}_3\text{NiSb}_{12}$); therefore, results of our tests recorded at about 500 HV can be ascribed to skutterudite. This attribution is confirmed by the observation that the distribution around 500 HV has the highest frequency, accounting for the predominance of the skutterudite phase within the samples.

Vickers microhardness of the skutteruditic phase was studied in more detail: in Figure 3 average values of microhardness of the only skutterudite in as-prepared samples, obtained by including only data centred around 500 HV in frequency distributions, is reported as a function of Fe amount: even if the range of the observed hardness values is restricted (it spans from 516 ± 5 for $x = 0.4$ to 447 ± 19 for $x = 1$) and data appear quite scattered, a substantial decrease can be observed with increasing the Fe amount. The hardness reduction reflects both the increase

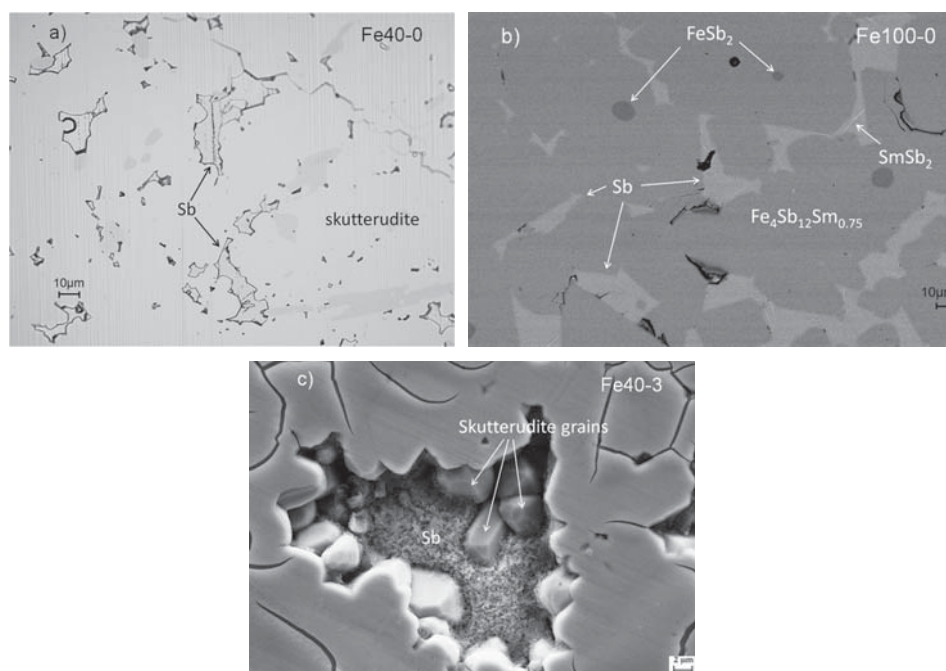


Figure 2. (a) Optical and (b) electronic micrograph (taken by backscattered electrons) of unetched Fe40-0 and Fe100-0 samples, respectively: the presence of Sb grains with well-defined shape is visible in both pictures. In picture (c) an electronic image (taken by secondary electrons) of the etched surface of sample Fe40-3 is shown. The presence of skutterudite crystals growing within the Sb-based matrix is visible.

in the Fe/Ni average atomic size and the decrease in the average atomic mass, as already stated in other studies.²¹ Owing to the fact that Fe/Ni skutterudites with $x > \sim 0.60$ are characterized by the p -type conduction mechanism, it can be concluded that p -skutterudites are less hard than n -type ones.

As aforementioned, values of microhardness clustering around 120 HV have been observed in some samples. Basing on the results of microhardness tests performed on Sb grains evidenced by etching, that provide HV values ranging from 110 to 130, the distribution centred at 120 HV has

been attributed to this additional phase. It is noteworthy that microhardness tests performed on a polished surface of pure Sb provided an average HV value of 70 HV, in agreement with values reported for pure Sb (50–70 HV).²⁴ The non negligible discrepancy between microhardness of pure Sb and Sb found as additional phase, is related to the hardening effect due to the presence of a certain amount of Fe/Ni and/or Sm dissolved within the Sb lattice, as indicated by EDS analyses.

As previously described, the presence of the Sb-rich solid solution at the skutterudite grain boundaries is expected, owing to the synthetic method, and it could be experimentally observed. The presence of this phase can explain the occurrence of the hardness distribution peak at ~ 350 HV, that most likely derives from measurements carried out on indentations involving both phases, that due to the remarkable difference between hardness of Sb and skutterudite, provide intermediate values.

The analysis of microhardness data collected on samples that underwent thermal treatments gives further hints about the formation mechanism of the skutterudite phase and can be interpreted in the light of the presence of a Sb-rich phase at the grain boundaries. Two main effects can be in fact observed in the microhardness behaviour as a consequence of thermal cycles:

(a) The frequency distribution at ~ 500 HV narrows, and the one at ~ 350 HV becomes less represented with increasing the number of thermal cycles. These trends are

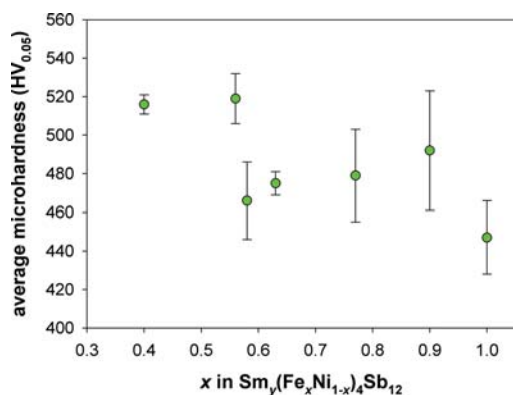


Figure 3. Vickers microhardness of as-prepared samples as a function of the Fe amount.

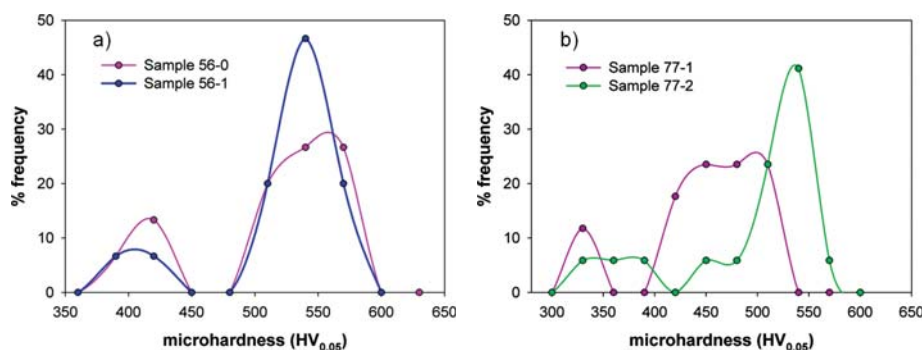


Figure 4. Microhardness frequency distribution of samples (a) Fe56-0 and Fe56-1, and (b) Fe77-1 and Fe77-2.

shown in Figure 4, where the hardness distributions of samples Fe56 and Fe77 are reported.

(b) Microhardness values of the skutteruditic phase increase with increasing the number of thermal cycles, as observable in Figure 5, where average HV values of samples Fe77 are reported as a function of the number of thermal treatments.

The described narrowing of the hardness distribution at ~ 500 HV reflects a drop in the scattering degree of hardness data (confirmed by the reduction of the error bar with increasing number of thermal treatments, see Fig. 5): it is a consequence of the phase homogenization induced by thermal treatments. At the same time, the decrease of the peak height of the distribution at ~ 350 HV suggests a reduction of the Sb-based phase amount at the grain boundaries. It has to be in fact considered that thermal treatments are supposed to cause a grain enlargement. Figure 6 shows for example electronic micrographs of samples Fe40-0 and Fe40-3 after etching, that highlight the grain growth occurring with thermal treatments: average grains sizes change from $\sim 6\text{--}10\ \mu\text{m}$ (Fe40-0) to $\sim 12\text{--}20\ \mu\text{m}$ (Fe40-3). A grain enlargement is generally expected to decrease the hardness of the phase; nevertheless, as previously described, all the samples analyzed

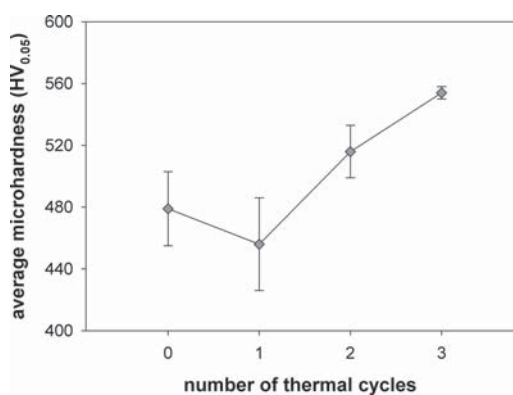


Figure 5. Vickers microhardness of sample Fe77 as a function of the thermal cycles number.

show a hardening of the skutterudite phase with increasing the number of thermal treatments. This evidence can be explained by taking into account that the grain growth occurs along with consumption of the Sb-based solid solution located at the grain boundary, as also suggested by the drop of height of the distribution peak at ~ 350 HV. EDS analyses performed close to the grain centre and to the grain border confirm a not negligibly higher Sb amount in the latter area (~ 78 at.%) than in the former (~ 76 at.%). Therefore, the hardness increase associated to thermal treatments points to a Sb enrichment of skutterudite.

The observed increase in the Sb amount within the skutterudite phase provides hints for the improvement of the

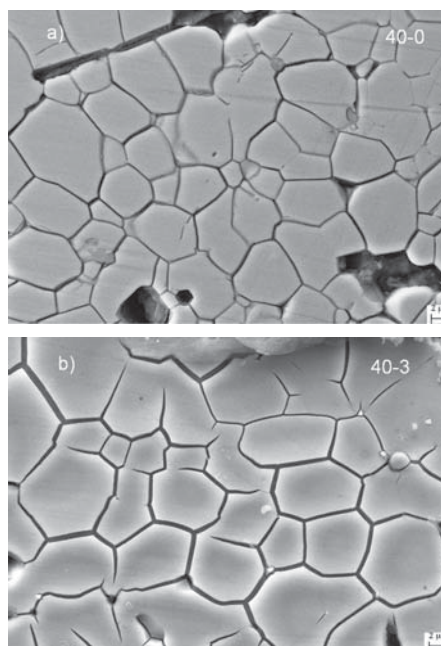


Figure 6. Electronic micrographs (taken by secondary electrons) of etched (a) 40-0 and (b) 40-3 samples. Grain boundaries are clearly visible; a significant grain growth can be observed with increasing the number of thermal cycles.

synthetic process. It indicates in fact that the treatment at 400 °C is for the obtainment of a Sb amount within the skutterudite close to the stoichiometric one. The initial treatment at 950 °C provides in fact a mixture of a Sb-based phase and $(\text{Fe,Ni})\text{Sb}_2$, and the subsequent treatment at 620 °C promotes the formation of the skutterudite through a peritectic reaction. Nevertheless, due to the high value of the Sb vapour pressure (10^{-3} mm Hg at 600 °C²⁵), Sb evaporation and diffusion are competitive phenomena at the treatment temperature, as proven by the less than stoichiometric value of the Sb amount obtained from Rietveld refinements (see Table I). Thus, the thermal treatment at 620 °C, necessary for the phase formation, should be properly followed by a treatment at lower temperature, with the aim to favour the Sb diffusion into the skutterudite grains, as well as the recovery of stresses existing in as-cast samples.

As grain enlargement and Sb enrichment act on the microhardness behaviour in opposite directions, it can be expected that after a higher number of thermal cycles, the softening due to grain growth starts prevailing over the hardening caused by the Sb enrichment.

4. CONCLUSIONS

A study of the Vickers microhardness behaviour of the filled skutterudite $\text{Sm}_y(\text{Fe}_x\text{Ni}_{1-x})_4\text{Sb}_{12}$ as a function of composition and number of thermal cycles, has been performed with the aim to evaluate the mechanical response of the material in conditions that simulate the operating ones. A dependence of microhardness on composition has been observed, since the average value related to the skutteruditic phase decreases with increasing the Fe amount, due to the increase of the mean Fe/Ni atomic size. Thermal cycles result in a drop of data scattering, due to the homogenization effect, and in a general hardness increase of skutterudite, as a consequence of the enrichment in Sb. The last point suggests also a possible improvement of the synthetic path, consisting in the introduction of a thermal treatment at low temperature in order to favour the Sb diffusion into the skutterudite grains rather than its evaporation.

Acknowledgments: Professor Paolo Piccardo (University of Genova) is kindly acknowledged for the helpful discussions; authors are grateful to Dr. Marcella Pani (University of Genova) for the critical revision of the manuscript.

References and Notes

1. B. Liu, X. Jia, D. Huo, H. Sun, Y. Zhang, B. Sun, H. Liu, L. Kong, and H. Ma, *J. Alloy Compd.* 666, 93 (2016).
2. R. Chetty, A. Bali, M. H. Naik, G. Rogl, P. Rogl, M. Jain, S. Suwas, and R. C. Mallik, *Acta Mater.* 100, 266 (2015).
3. R. Carlini, C. Artini, G. Borzone, R. Masini, G. Zanicchi, and G. A. Costa, *J. Therm. Anal. Calorim.* 103, 23 (2011).
4. B. C. Sales, Handbook on the Physics and Chemistry of Rare Earths, edited by K. A. Gschneidner, Jr., J.-C. G. Bünzli, and V. K. Pecharsky, North Holland, Amsterdam, New York, Oxford (2003), Vol. 33, p. 1.
5. C. Uher, Thermoelectrics Handbook—Macro to Nano, edited by D. M. Rowe, Taylor, and Francis, Boca Raton (2006), Vol. 34, p. 1.
6. H. Kitagawa, M. Hasaka, T. Morimura, H. Nakashima, and S. Kondo, *Mater. Res. Bull.* 35, 185 (2000).
7. Y. Dong, P. Puneet, T. M. Tritt, and G. S. Nolas, *J. Solid State Chem.* 209, 1 (2014).
8. A. Kaltzoglou, P. Vaquero, K. S. Knight, and A. V. Powell, *J. Solid State Chem.* 193, 36 (2012).
9. L. Chapon, D. Ravot, and J. C. Tedenac, *J. Alloy Compd.* 282, 58 (1999).
10. T. Morimura and M. Hasaka, *Scripta Mater.* 48, 495 (2003).
11. R. Carlini, A. U. Khan, R. Ricciardi, and T. Mori, *J. Alloy Compd.* 655, 321 (2016).
12. C. Artini, G. Zanicchi, G. A. Costa, M. M. Carnasciali, C. Fanciulli, and R. Carlini, *Inorg. Chem.* 55, 2574 (2016).
13. B. Bourgouin, D. Bérardan, E. Alleno, C. Godart, O. Rouleau, and E. Leroy, *J. Alloy Compd.* 399, 47 (2005).
14. D. Bérardan, E. Alleno, C. Godart, O. Rouleau, and J. Rodriguez-Carvajal, *Mater. Res. Bull.* 40, 537 (2005).
15. X. F. Tang, L. M. Zhang, R. Z. Yuan, L. D. Chen, T. Goto, T. Hirai, J. S. Dyck, W. Chen, and C. Uher, *J. Mater. Res.* 16, 3343 (2001).
16. X. Tang, L. Chen, T. Goto, and T. Hirai, *J. Mater. Res.* 16, 837 (2001).
17. I. Oftedal, *Z. Kristallogr. A* 66, 517 (1928).
18. W. Jeitschko and D. J. Braun, *Acta Cryst. B* 33, 3401 (1977).
19. B. C. Chakoumakos and B. C. Sales, *J. Alloy Compd.* 407, 87 (2006).
20. G. Rogl, A. Grytsiv, E. Royanian, P. Heinrich, E. Bauer, P. Rogl, M. Zehetbauer, S. Puchegger, M. Reinecker, and W. Schranz, *Acta Mater.* 61, 4066 (2013).
21. L. Zhang, G. Rogl, A. Grytsiv, S. Puchegger, J. Koppensteiner, F. Spieckermann, H. Kabelka, M. Reinecker, P. Rogl, W. Schranz, M. Zehetbauer, and M. A. Carpenter, *Mater. Sci. Eng. B* 170, 26 (2010).
22. G. Rogl, A. Grytsiv, E. Bauer, P. Rogl, and M. Zehetbauer, *Intermetallics* 18, 57 (2010).
23. V. Keppens, D. Mandrus, B. C. Sales, B. C. Chakoumakos, P. Dai, R. Coldea, M. B. Maple, D. A. Gajevski, E. J. Freeman, and S. Bennington, *Nature* 395, 876 (1998).
24. B. Lafuente, R. T. Downs, H. Yang, and N. Stone, Highlights in Mineralogical Crystallography, edited by T. Armbruster, R. M. Danisi, and W. De Gruyter, Berlin (2015), p. 1.
25. R. C. Weast (ed.), Handbook of Chemistry and Physics, CRC Press, Cleveland (1976), p. D-182.

Received: 25 February 2016. Accepted: 23 May 2016.